ISSN 1063-7710, Acoustical Physics, 2010, Vol. 56, No. 6, pp. 962–971. © Pleiades Publishing, Ltd., 2010.

Wave Radiation in Lattice Fracture[1]

L. I. Slepyan

School of Mechanical Engineering, Tel Aviv University, lsrael

e-mail: leonid@eng.tau.ac.il

Received February 17, 2010

Abstract—The square and triangular lattices are considered, where the uniform crack growth is accompanied by the wave radiation. The radiation energy and structure are studied. The energy radiated to the bulk of the lattice is found in a direct way. The radiation structure is described based on the crack problem solution and by means of the analysis of two-dimensional dispersion relations for the intact lattice. The mode III problem for square lattice is discussed in detail, whereas, in the case of the plane problem for the triangular lattice, the only those results are derived which follow from the two-dimensional dispersion relations. It is shown that there exists a finite crack-speed-dependent region of wavenumbers corresponding to the waves radiated to the bulk of the lattice. In the case of the triangular-cell lattice, in addition, one or several lattice Rayleigh waves are radiated. For the square lattice a complete solution for the wave field is presented with the crack-speed-dependent far-field asymptote. The latter is characterized by the wave amplitude asymptotically decreasing as the distance from the crack front in power $-1/3$. The asymptotically significant crack-speed-dependent direction of the radiation is determined. Such asymptotic results are also valid for the triangular lattice.

DOI: 10.1134/S1063771010060217

1. INTRODUCTION

The classical continuum model of the material can be considered only as the slowly-varying approximation of a discrete or structured material. This accuracy is sufficient for the analysis of regular processes in which waves corresponding to the microstructural scales can be neglected. However, macro-processes exist, and they are not a rarity in nature, when the asymptotic approximation of this kind is not sufficient. Fracture is an excellent example of such a process. The energy release through the propagating crack tip imposes no lower limit of the wave length, and the characteristic size related to the microstructure cannot be neglected. Under the microstructural influence a great part of the macrolevel energy release is spent on the excitation of the microlevel and this phenomenon cannot be observed within the framework of the homogeneous model. The discrete lattice model helps to illuminate the energy release process, accompanied by the high-frequency wave radiation, and to reveal the other phenomena accompanying crack propagation in a structured medium.

Analytical studies of fracture using lattice models began with the works by Slepyan (1981a, 1981b), where a massless-bond, discrete, square-cell lattice was considered. In these papers, steady-state mode III dynamic problem for a semi-infinite crack uniformly growing in the unbounded lattice was examined. Such but a triangular-cell lattice was considered in Kulakhmetova et al. (1984). Main analytical works in this topic are summarized in the book by Slepyan (2002). Contrary to the elastic continuum the lattice admits waves with reduced phase speeds, and these waves are excited by the uniformly growing crack. The radiation increases much the total fracture energy, and the determination of the latter as a function of the crack speed was the main purpose of the analysis. The radiation energy strongly depends on the crack speed and it does not vanishes as the latter tends to zero. Some aspects of wave radiation of the propagating crack were discussed in Slepyan (1981b, 2002), Mishuris et al. (2009) and Slepyan et al. (2009).

Note that, in the lattice model, similar phenomena in fracture and phase-transitions are revealed. A phase-transition wave in a discrete chain consisting of bistable irreversible elements was first considered by Slepyan and Troyankina (1984) [also see Slepyan and Ayzenberg-Stepanenko (2004), Cherkaev et al. (2005), Slepyan et al. (2005), Vainchtein (2010), and the references herein].

In the present paper, the waves radiated by a crack uniformly propagating in square and triangular lattices are studied. The mode III problem for square lattice is considered in detail. The total energy of the radiation is obtained as the local-to-global energy release ratio. The energy radiated to the bulk of the lattice is found by a direct way. In the case of the square lattice, where no localized wave exists, these two approaches yield the same result. The radiation structure is studied by means of the analysis of two-dimensional dispersion relations for the unbounded lattice and the lattice half-plane. It is shown, in particular, that there exists a

[1] The article is published in the original.

finite crack-speed-dependent region of wavenumbers corresponding to the waves radiated to the bulk of the lattice. In addition, in the case of the triangular-cell lattice, one or several lattice Rayleigh waves localized at the crack faces are radiated. For the square lattice a complete solution for the wave field is presented with the far-field asymptote. The asymptotically significant crack-speed-dependent direction of the radiation is determined.

2. MODE III FRACTURE IN A SQUARE-CELL LATTICE

2.1. Formulation and General Solution in Outline

Consider an infinite lattice consisting of point particles of mass M. Each particle is connected with four neighbors by the same linearly elastic bonds each of length a (Fig. 1). For this lattice mode III crack propagation is studied. A semi-infinite crack is assumed to propagate to the right with constant speed v; that is, the time-interval between the breakage of neighboring bonds on the crack path, a/v, is constant. In this "steady-state" process, a part of the energy, delivered by a *feeding wave* from a remote source, is spent on the bond disintegration on the crack path and the rest is radiated away from the crack front. The dynamic equation of the lattice for the anti-plane strain is a discrete analogue of the two-dimensional wave equation

$$M\frac{\mathrm{d}^2 u_{m,n}(t)}{\mathrm{d}t^2} = \mu[u_{m+1,n}(t) + u_{m-1,n}(t) + u_{m,n+1}(t) + u_{m,n-1}(t) - 4u_{m,n}(t)], \quad (1)$$

where $u_{m,n}(t)$ are displacements, m and n are discrete coordinates of the particles, Fig. 1, and μ is the bond stiffness.

Via a long-wave approximation, the lattice corresponds to a homogeneous body of density M/a^2 and shear modulus μ (the lattice is assumed to be of a unit thickness). Accordingly, the shear wave velocity is given by $c = c_2 = \sqrt{a^2\mu/M}$. A subcritical crack speed is assumed: $0 < v < c_2$. In the following, μ, M and a are assumed to be the natural units; in these terms, $c_2 = 1$.

For the considered steady-state problem a moving coordinate, $\eta = m - vt$ is introduced. Assuming $u_{m,n}(t) = u_n(\eta)$ equation (1) can be rewritten in the form

$$v^2\frac{\mathrm{d}^2 u_n(\eta)}{\mathrm{d}\eta^2} = u_n(\eta+1) + u_n(\eta-1) + u_{n+1}(\eta) + u_{n-1}(\eta) - 4u_n(\eta). \quad (2)$$

The Fourier transform on η for $n \ge 0$ leads to a general solution of the form

$$u_n^F(k) = u^F(k)\lambda^n(k), \quad (3)$$

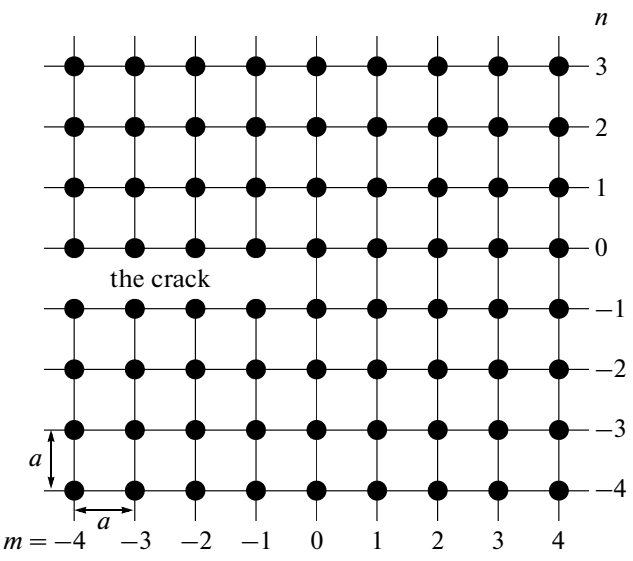

Fig. 1. The square-cell lattice.

with

$$u(\eta) = u_0(\eta), \quad \lambda(k) = \frac{r(k) - h(k)}{r(k) + h(k)} \quad (|\lambda| \le 1), \quad (4)$$

$$h^2(k) = 2(1 - \cos k) + (0 + \mathrm{i}kv)^2, \quad r^2(k) = h^2 + 4,$$

where, in accordance with the causality principle for steady-state solutions (see Slepyan (2002)), it is written $0 + \mathrm{i}kv = \lim_{s \to +0}(s + \mathrm{i}kv)$ instead of $\mathrm{i}kv$.

The antisymmetric problem is considered, $u_{-n}(\eta) = -u_{n-1}$, $n = 1, 2, \ldots$ In terms of the Fourier transform, Eq. (2) yields

$$\frac{r(r^2 - rh - 2)}{r + h}u^F(k) = 0. \quad (5)$$

This equation is valid for the intact lattice. It is, however, assumed that there is a crack, where there is no interaction between the lines of the particles $n = 0$ and $n = -1$ at $\eta < 0$. To take this into account the external forces compensating the interaction must be introduced in (2) for $\eta < 0$. In terms of the Fourier transform, equation (5) becomes

$$\frac{r(r^2 - rh - 2)}{r + h}u^F(k) = 2u_-(k), \quad (6)$$

where

$$u^F(k) = u_+ + u_-, \quad u_\pm = \int_{0(-\infty)}^{\infty(0)} u(\eta)\mathrm{e}^{\mathrm{i}k\eta}\mathrm{d}\eta. \quad (7)$$

Equation (6) yields the Wiener–Hopf type equation:

$$u_+(k) + L(k)u_-(k) = 0, \quad L(k) = \frac{h(k)}{r(k)}. \quad (8)$$

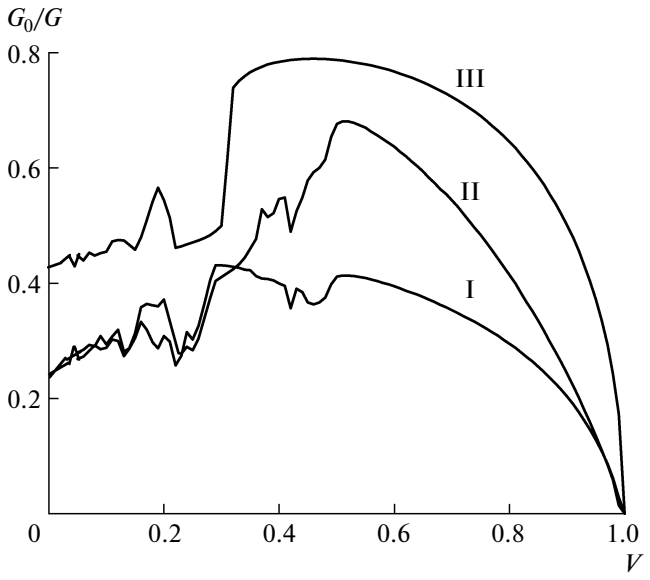

Fig. 2. Energy release ratios, G_0/G: (I) Mode I ($V = v/c_R$); (II) Mode II ($V = v/c_R$); (III) Mode III ($V = v/c_2$).

The Wiener–Hopf technique is based on the factorization, $L(k) = L_+(k)L_-(k)$, that can be achieved using the Cauchy-type integral:

$$L_\pm(k) = \exp\left[\pm\frac{1}{2\pi i}\int_{-\infty}^{\infty}\frac{\ln L(\xi)}{\xi - k}d\xi\right], \quad \pm\Im k > 0. \quad (9)$$

Here $L_+(k)$ is a regular function in the upper half-plane, and $L_-(k)$ is a regular function in the lower half-plane; $L_\pm(\pm i\infty) = 1$. In this way, it is convenient to normalize the kernel $L(k)$, that is to separate zeros of $h(k)$ and $r(k)$. For $v > v_*$, $v_* \approx 0.315847$, such a normalization is

$$L^2(k) = \frac{(0+ik)(0-ik)(0+i(k-h_1)(0+i(k+h_1)}{(1+k^2)(0+i(k-r_1)(0+i(k+r_1)}S^2(k), \quad (10)$$

where h_1, r_1 are the roots: $h(\pm h_1) = r(\pm r_1) = 0$ (the number of roots grows as the speed v decreases). In this representation, $S(k) > 0$. It follows that

$$L_+(k) = \sqrt{\frac{0-ik}{1-ik}}S_+(k),$$

$$L_-(k) = \sqrt{\frac{(0+ik)(0+i(k-h_1))(0+i(k+h_1))}{(1+ik)(0+i(k-r_1))(0+i(k+r_1))}}S_-(k),$$

$$S\pm(k) = \sqrt{S(k)}\exp\left[\pm\frac{1}{2\pi i}\text{V.p.}\int_{-\infty}^{\infty}\frac{\ln S(\xi)}{\xi - k}d\xi\right], \quad (11)$$

$$\Im k = 0.$$

Equation (8) is now represented as

$$\frac{u_+(k)}{L_+(k)} + L_-(k)u_-(k) = A\left(\frac{1}{0+ik} + \frac{1}{0-ik}\right), \quad (12)$$

where an analytical representation of the delta function of k is introduced in the right-hand side. This reflects a remote constant load; A is an arbitrary constant. The representation corresponds to the *macrolevel-associated solution*, where the energy is delivered to the moving crack front by a non-oscillating wave. Note that the *microlevel-associated solutions*, where the energy is delivered by an oscillating feeding wave, also exist (see Slepyan (2002)). Finally, the solution is

$$u_+(k) = \frac{AL_+(k)}{0-ik}, \quad u_-(k) = \frac{A}{L_-(k)(0+ik)}. \quad (13)$$

2.2. The Radiation Energy

Let σ_c be the critical tensile force of the bond. Then

$$u(0) = \lim_{s\to\infty} su_+(is) = A = \frac{\sigma_c}{2}. \quad (14)$$

This relation defines the constant A. Thus the fracture energy itself as the critical strain energy of the breaking bonds per unit length is

$$G_0 = \sigma_c u(0) = 2A^2. \quad (15)$$

At the same time, the macrolevel energy release rate, G, is defined by the long-wave approximation of the solution, which corresponds to the continuous analogue of the lattice; it can be obtained from (13) as an asymptote, $k \to 0$. In this way, it is found that (see Slepyan (1981a), (2002))

$$G = G_0\mathcal{R}^{-1}(v), \quad \mathcal{R}(v) = \exp\left[-\frac{2}{\pi}\int_0^{\infty}\frac{\text{Arg}\,L(k)}{k}dk\right] = \prod_{\nu=1,3,\ldots}\frac{h_\nu}{r_\nu}\prod_{\nu=2,4,\ldots}\frac{r_\nu}{h_\nu}, \quad (16)$$

where for $v > 0$ there is a finite set of the roots, (h_ν, r_ν): $h(h_\nu) = 0$, $r(r_\nu) = 0$ ($h_{\nu+1} \geq h_\nu$ and $r_{\nu+1} \geq r_\nu$). In particular, $\mathcal{R} = h_1/r_1$ for $v > v_*$. Note that for a vanishing speed

$$\mathcal{R}(+0) = \exp\left[-\frac{1}{2\pi}\int_0^{\pi}\ln\frac{4+2(1-\cos k)}{2(1-\cos k)}dk\right] = \sqrt{2}-1. \quad (17)$$

The crack speed-dependent energy ratio $G_0/G = \mathcal{R}(v)$ is presented in Fig. 2 for each of three fracture modes, where modes I and II correspond to the plane problem

for the triangular lattice (in this case, v is the ratio of the crack speed to the long Rayleigh wave speed).

The normalized difference

$$R(v) = \frac{G - G_0}{G} = 1 - \mathcal{R}(v) \tag{18}$$

corresponds to the radiated energy. No surface wave exists in the square lattice half-plane; hence all this energy must be radiated to the bulk of the lattice. This statement is proved below by means of a direct determination of the energy flux radiated to $n \to \infty$.

2.3. Structure of the Radiation

2.3.1. Energy radiated to the bulk of the lattice. The radiation structure can be disclosed using a direct way of the energy flux determination. The total energy flux from the node (m, n) to the node $(m, n+1)$ is

$$G_r = G_{n \to n+1} = \int_{-\infty}^{\infty} [u_{m,n}(t) - u_{m,n+1}(t)]\dot{u}_{m,n+1}(t)\mathrm{d}t. \tag{19}$$

Note that the result is independent of m. Using the Parseval identity and taking into account that

$$u^F_{n+1}(k) = u^F_n(k)\lambda(k) = u^F(k)\lambda^{n+1}(k) \quad (n \geq 0) \tag{20}$$

equality (19) can be expressed in the form

$$G_r = -\int_{-\infty}^{\infty} [u_n(\eta) - u_{n+1}(\eta)]\frac{\mathrm{d}u_{n+1}(\eta)}{\mathrm{d}\eta}\mathrm{d}\eta$$

$$= -\frac{1}{2\pi}\int_{-\infty}^{\infty} [u^F_n(k) - u^F_{n+1}(k)]\overline{(-\mathrm{i}k)u^F_{n+1}(k)}\mathrm{d}k \tag{21}$$

$$= -\frac{1}{2\pi}\int_{-\infty}^{\infty} |u^F(k)|^2[1 - \lambda(k)]|\lambda|^{2n}\overline{(-\mathrm{i}k)\lambda(k)}\mathrm{d}k,$$

where the pole at $k = 0$, corresponding to the feeding wave, must be ignored. Only the segments where $\lambda(k)$ is complex give a contribution to the integral (21). In this domain

$$|\lambda(k)| = 1, \quad \Im\lambda(k) = -\frac{1}{2}r(k)\sqrt{-h^2(k)} \quad (h^2 < 0), \tag{22}$$

and it follows that

$$G_r = \frac{1}{2\pi}\int_{\mathcal{H}} |u^F(k)|^2 r(k)\sqrt{-h^2(k)}k\mathrm{d}k, \tag{23}$$

where the domain $\mathcal{H}$ is a subset of the positive semi-axis $k > 0$, where $\Im\lambda \neq 0$, that is where

$$-4 < h^2(k) < 0 \quad (h^2 < 0, r^2 > 0). \tag{24}$$

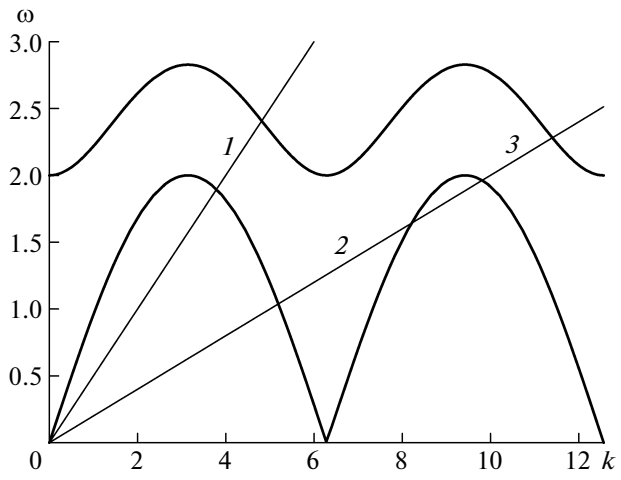

Fig. 3. The dispersion curves, $\omega = \omega_h$ (the lower curve) and $\omega = \omega_r$ (the upper curve), and the rays $\omega = 0.5k$ and $\omega = 0.2k$. The segments corresponding to the radiation ($\mathcal{H}$-segments): (*1*) $3.791 < k < 4.815$ for $v = 0.5$; (*2*) $5.1915 < k < 8.2092$ and (*3*) $9.8126 < k < 11.4053$ for $v = 0.2$.

The ratio of the radiated energy to the total energy release rate is

$$R = \frac{2G_r}{G} = \frac{2G_r\mathcal{R}}{G_0} = \frac{\mathcal{R}}{2\pi}\int_{\mathcal{H}} \left|\frac{1 - L(k)}{L_-(k)}\right|^2 r(k)\sqrt{-h^2(k)}\frac{\mathrm{d}k}{k}, \tag{25}$$

and the corresponding wave numbers are situated in the regions where $-4 < h^2 < 0$ (24). These regions can be seen in Fig. 3, where dispersion relations, following from equations $h(k) = 0$ and $r(k) = 0$

$$\omega = \omega_h = \pm 2\sin k/2, \quad \omega = \omega_r = \pm 2\sqrt{1 + \sin^2 k/2}, \tag{26}$$

and the rays $\omega = kv$ are shown in the first quadrant of the k, ω-plane. Note that there exists only a single $\mathcal{H}$-segment at $k > 0$ for $v > v_*$. It follows from (25), (11) and (16) that, in this case

$$R = \frac{2\mathcal{R}}{\pi}\int_{h_1}^{r_1} \sqrt{\frac{r_1^2 - k^2}{k^2 - h_1^2}}\frac{\mathrm{d}k}{k} = \mathcal{R}\left(\frac{r_1}{h_1} - 1\right) = 1 - \mathcal{R}. \tag{27}$$

Thus, the energy is completely radiated to the bulk of the lattice, as it should be.

2.3.2. Two-dimensional dispersion relation and the radiation. Now consider the two-dimensional dispersion relation following from the lattice dynamic equation (1) for the sinusoidal wave

$$u_{m,n} = \exp[\mathrm{i}(\omega t - km - qn)]. \tag{28}$$

It is

$$\omega = \pm\sqrt{4 - 2\cos k - 2\cos q}, \quad -\pi < q \le \pi. \qquad (29)$$

In the steady-state problem, the radiated wave frequency and the crack speed are connected by the relation as

$$\omega = kv. \qquad (30)$$

It is important that this relation is valid not only for the main k-range, $-\pi < k \le \pi$, but for the periodic continuation of the dispersion relation, that is for $-\infty < k < \infty$. For a given values of $\omega \in (0, \sqrt{8})$ and $k = k_0 \in (-\pi, \pi)$, the relation is valid for $v = \omega/(k_0 \pm 2\pi\nu)$, $\nu = 0, \pm 1, \ldots$. If v is given, one or several couples, ω, k, are defined by the dispersion relation and the steady-state condition (30). With this in mind, here the ratio ω/k is called the phase speed for any $k \in (-\infty, \infty)$. Note that the group velocity and the particle motion are independent of the value of integer ν in the above relation. It follows from (29) and (30) that

$$-4 \le 2(1 - \cos k) - k^2 v^2 \le 0, \qquad (31)$$

and this coincides with the definition of the $\mathcal{K}$-segments (24). The phase velocity as a vector, $\mathbf{V}$, is

$$|\mathbf{V}| = \frac{\omega}{\sqrt{k^2 + q^2}}, \quad V_x = \frac{\omega k}{k^2 + q^2}, \quad V_y = \frac{\omega q}{k^2 + q^2}. \qquad (32)$$

The group velocity vector, $\mathbf{V_g}$, is

$$|\mathbf{V_g}| = \frac{\sqrt{\sin^2 k + \sin^2 q}}{\omega}, \qquad (33)$$
$$(V_g)_x = \frac{\sin k}{\omega}, \quad (V_g)_y = \frac{\sin q}{\omega}.$$

For the radiated waves these relations are valid with $\omega = kv$, and if q is defined as a non-negative value

$$q = \arccos(2 - \cos k - k^2 v^2/2) \ge 0, \qquad (34)$$

then for k in the segments defined in (31)

$$V_x = \frac{vk^2}{k^2 + q^2}, \quad V_y = \mp\frac{vkq}{k^2 + q^2}, \qquad (35)$$
$$(V_g)_x = \frac{\sin k}{vk}, \quad (V_g)_y = \pm\frac{\sin q}{vk},$$

in the upper and lower lattice half-planes, respectively.

2.4. The Far Field Asymptote

The wave field in the upper lattice half-plane is defined by the inverse Fourier transform

$$u_n(\eta) = \frac{1}{2\pi}\int_{-\infty}^{\infty}[u_+(k) + u_-(k)]\lambda^n \exp(-ik\eta). \qquad (36)$$

It follows from (13) and (4), where for the radiated waves $|\lambda| = 1$, that the field far from the crack front can be represented as

$$u_n(\eta) = A\Im U,$$

$$U = \frac{1}{\pi}\int_{\mathcal{H}}\frac{1 - L(k)}{L_-(k)}\exp[-i(Q(k)n + k\eta)]\frac{dk}{k}, \qquad (37)$$

$$Q(k) = 2\arctan\sqrt{\frac{-h^2}{r^2}} = \arccos\left(1 + \frac{1}{2}h^2(k)\right).$$

For the asymptotic analysis of the integral it is important that in the range $0.315847 < v < 1$, where there is only a single positive $\mathcal{H}$-segment, there exists a point $k = k_*(v) \in \mathcal{H}$ where

$$\frac{d^2Q(k)}{dk^2} = 0, \quad P(k) = \frac{d^3Q(k)}{dk^3} > 0 \quad (k = k_*(v)). \qquad (38)$$

This point defines the ray

$$\eta = \eta_* = -\frac{dQ(k)}{dk}n \quad (k = k_*(v)), \qquad (39)$$

where the wave amplitude decreases as $n^{-1/3}$, while on the other rays, it decreases as $1/\sqrt{n}$. The contribution of this point for $n \to \infty$ can be expressed as

$$U \sim \frac{2[1 - L(k_*(v))]}{k_*(v)L_-(k_*(v))}\exp[-i(Q(k_*)n + k_*\eta)]I,$$

$$I = \frac{1}{\pi}\int_0^\infty \cos\left[\frac{1}{6}P(k_*(v))t^3 n + t\eta'\right]dt \qquad (40)$$
$$= [P(k_*(v))n/2]^{-1/3}\mathrm{AiryAi}(\kappa(v)),$$

$$\mathrm{AiryAi}(x) = \frac{1}{\pi}\int_0^\infty \cos\left(\frac{1}{3}t^3 + xt\right)dt,$$

where $\kappa(v) = \eta'[(P(k_*(v))n/2]^{-1/3}$ and $\eta' = \eta - \eta_*[\mathrm{AiryAi}(0) = 3^{-2/3}/\Gamma(2/3)]$.

The Airy function in a vicinity of $\eta' = 0$, is shown in Fig. 4. The plot of the wavenumber $k_*(v)$, corresponding to the main far-field asymptote of the radiation, is presented in Fig. 5. The main asymptote ray definition, $-\eta/n = dQ/dk$ $(k = k_*)$ is plotted in Fig. 6. The functions $Q(k_*)$ and $P(k_*)$ are shown in Figs. 7 and 8, respectively.

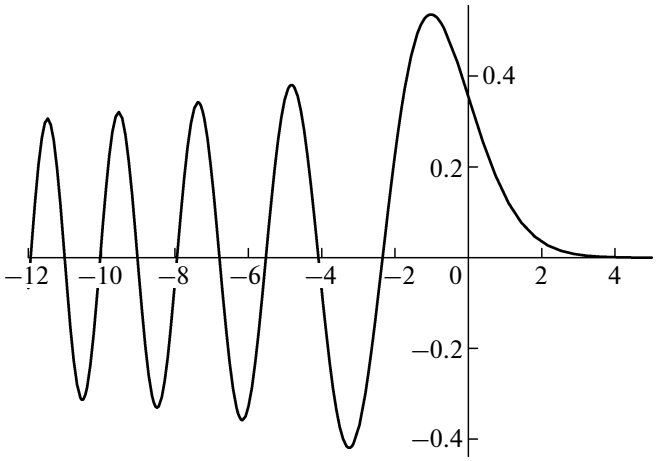

Fig. 4. The envelope of the main asymptote in a vicinity of the ray $\eta = \eta_*(n)$: The Airy function, AiryAi(x).

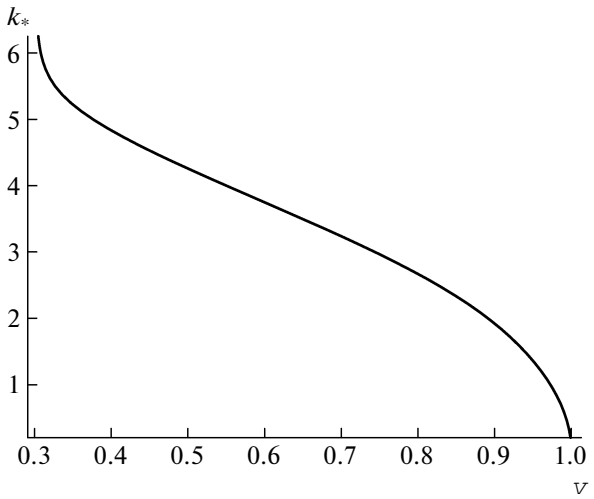

Fig. 5. The asymptote-related wavenumber as a function of the crack speed.

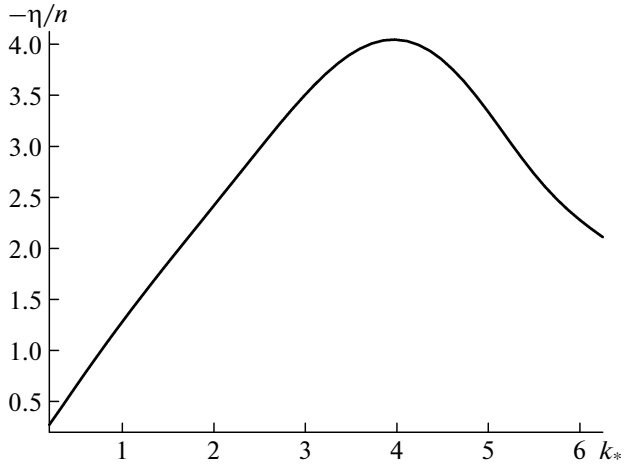

Fig. 6. The main ray of the radiation, $\eta/n = -\mathrm{d}Q/\mathrm{d}k$ ($k = k_*$), as a function of $k_*(v)$.

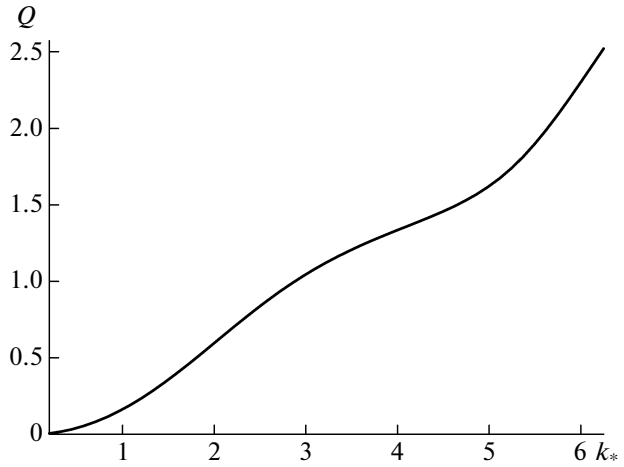

Fig. 7. The function $Q(k)$.

3. TRIANGULAR-CELL LATTICE

3.1. The Lattice

For the triangular lattice, where the plane problem is considered, the analysis is based only on the dispersion relations. In this lattice, each particle of mass M is connected with six neighbors by the same elastic bonds, each of the length a and stiffness μ. In the long-wave approximation, the lattice corresponds to a homogeneous, isotropic, elastic body with density $\rho = 2M/(\sqrt{3}\,a^2)$, Poisson's ratio $\nu = 1/3$ and the following velocities of the longitudinal, shear and Rayleigh waves: $c_1 = \sqrt{9/8}\,c$, $c_2 = \sqrt{3/8}\,c$ and $c_R = 1/2\sqrt{3-\sqrt{3}}\,c$, respectively, where $c = \sqrt{a^2\mu/M}$. The shear modulus is $\mu_0 = \rho c_2^2 = \sqrt{3}\,\mu/4$.

In the following, non-dimensional values associated with the natural units are used: the particle mass ($M = 1$), the bond length ($a = 1$) and the bond stiffness ($\mu = 1$). In these terms, c is the speed unit ($c = 1$), a/c is the time unit, $\rho = 2/\sqrt{3}$, $c_1 = \sqrt{9/8}$, $c_2 = \sqrt{3/8}$ and $c_R = 1/2\sqrt{3-\sqrt{3}}$.

Coordinates of the particles are defined by integers (m, n) or by the vector $\mathbf{x}$ which rectangular coordinates x, y are

$$x = m + n/2, \quad y = \frac{\sqrt{3}}{2}n, \quad m, n = 0, \pm 1, \pm 2, \ldots. \quad (41)$$

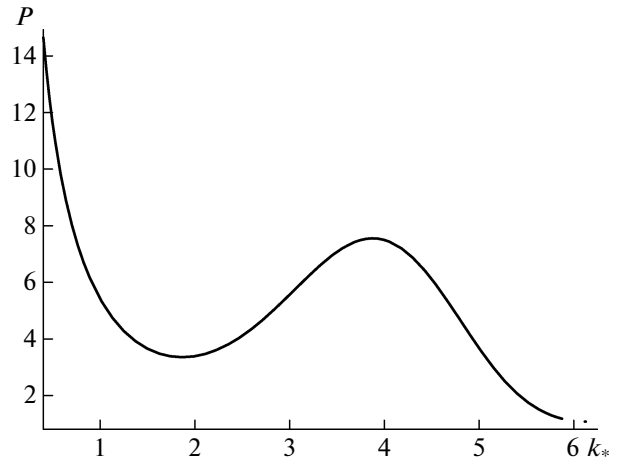

Fig. 8. The function $P(k)$.

Crack propagation is a consequence of disintegration of the bonds between lines $n = 0$ and $n = -1$. The lattice and the unit vectors, introduced below, are shown in Fig. 9.

3.2. Dynamic Equations

Unite vectors $\mathbf{I}_i$, $i = 0, 1, ..., 5$, directed from a given particle to the neighbors are introduced. In terms of the projections onto x, y-axes, these vectors are

$$\mathbf{I}_i = [\cos(\pi i/3), \sin(\pi i/3)], \quad i = 0, 1, \ldots, 5. \quad (42)$$

The dynamic equation for a particle outside the crack is

$$\frac{d^2\mathbf{u}(t, \mathbf{x})}{dt^2} - \sum_{i=0}^{5} Q_i(t, \mathbf{x})\mathbf{I}_i = 0, \quad (43)$$

where $\mathbf{u}(t, \mathbf{x})$ is the displacement vector and $Q_i(t, \mathbf{x})$ is the elongation of the bond associated with vector $\mathbf{I}_i$:

$$Q_i(t, \mathbf{x}) = [\mathbf{u}(t, \mathbf{x} + \mathbf{I}_i) - \mathbf{u}(t, \mathbf{x})]\mathbf{I}_i. \quad (44)$$

For the considered steady-state problem, the displacements are assumed to depend on $\eta = x - vt$ and y for $x = m + n/2$ and $y = \sqrt{3}\, n/2$, that is, $\mathbf{u} = \mathbf{u}(\mathbf{X})$, $\mathbf{X} = (\eta, \sqrt{3}\, n/2)$. The equation of motion becomes

$$v^2\frac{d^2\mathbf{u}(\mathbf{X})}{d\eta^2} - \sum_{i=0}^{5} Q_i(\mathbf{X})\mathbf{I}_i = 0,$$
$$Q_i(\mathbf{X}) = [\mathbf{u}(\mathbf{X} + \mathbf{I}_i) - \mathbf{u}(\mathbf{X})]\mathbf{I}_i. \quad (45)$$

3.3. Dispersion Relations

For the sinusoidal wave

$$\mathbf{u}(t, \mathbf{x}) = \exp[\mathrm{i}(\omega t - kx - qy)] \quad (46)$$

in the unbounded lattice, equation (45) yields a two-dimensional dispersion relation

$$(\omega^2 - 3 + 2\cos(k) + \cos(k/2)\cos(\sqrt{3}q/2))$$
$$\times (\omega^2 - 3 + 3\cos(k/2)\cos(\sqrt{3}q/2)) \quad (47)$$
$$- 3\sin^2(k/2)\sin^2(\sqrt{3}q/2) = 0.$$

In particular, for $q = 0$ and $q = 2\pi/\sqrt{3}$, four dispersion relations follow as

$$\omega = \omega_1(k) = \pm\sqrt{3 - 2\cos(k) - \cos(k/2)},$$
$$\omega = \omega_2(k) = \pm\sqrt{6}\cos(k/4) \quad (q = 0),$$
$$\omega = \omega_3(k) = \omega_1(k + 2\pi), \quad (48)$$
$$\omega = \omega_4(k) = \omega_2(k + 2\pi) \quad (q = 2\pi/\sqrt{3}).$$

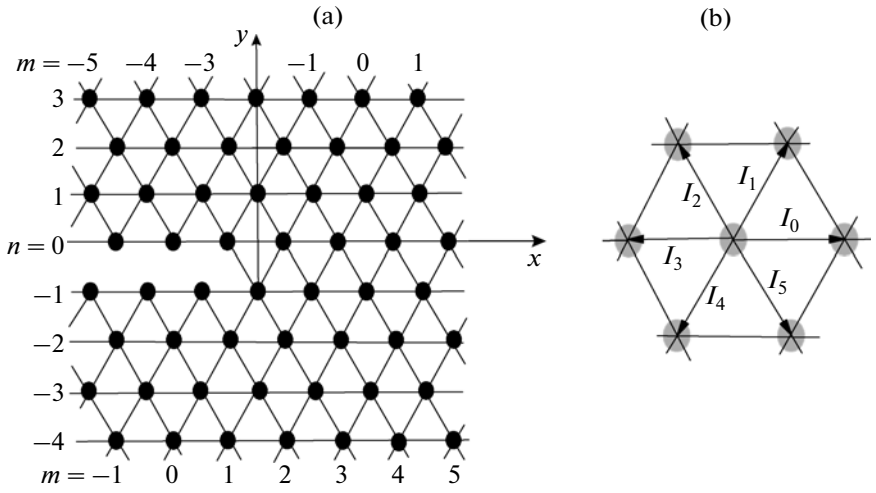

Fig. 9. The triangular-cell lattice: (a) the lattice and the coordinates; (b) the unit vectors.

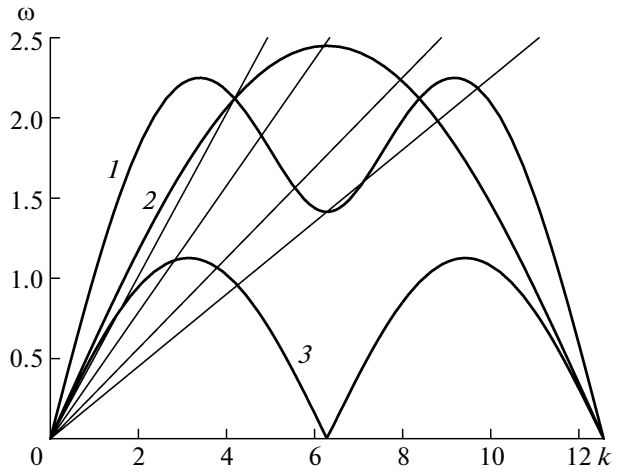

Fig. 10. The dispersion relations for the triangular-cell lattice: $\omega = \omega_1$ (*1*), $\omega = \omega_2$ (*2*), $\omega = \omega_R$ (*3*), and the rays $\omega = 0.4c_Rk$, $\omega = 0.5c_Rk$, $\omega = 0.7c_Rk$, $\omega = 0.9c_Rk$.

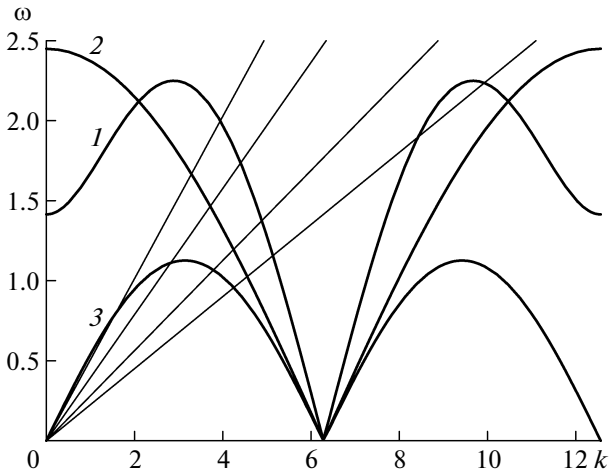

Fig. 11. The dispersion relations for the triangular-cell lattice: $\omega = \omega_3$ (*1*), $\omega = \omega_4$ (*2*), $\omega = \omega_R$ (3), and the rays $\omega = 0.4c_Rk$, $\omega = 0.5c_Rk$, $\omega = 0.7c_Rk$, $\omega = 0.9c_R/k$.

In the lattice half-plane with the x-axis as the boundary, there exists the lattice Rayleigh wave which amplitude exponentially decreases with the distance from the half-plane boundary. The corresponding dispersion relation is

$$\omega_R = \pm 2c_R|\sin(k/2)|. \quad (49)$$

The dispersion curves, $\omega_1(k)$, ... $\omega_4(k)$ and ω_R, in the first quadrant of the k, ω-plane, are plotted in Figs. 10 and 11.

3.4. Structure of the Radiation

The propagating crack can excite waves which phase speed along the x-axis coincides with the crack speed (see Section 2.3.2). In the triangular lattice, the radiation consists of the lattice Rayleigh wave (see (49) and Fig. 10) and the waves radiated to the bulk of the lattice. The crack-speed-dependent k-regions of the radiation follows from the dependence of $\cos(\sqrt{3}\,q/2)$ on real k as in the dispersion relation (47) with $\omega = kv$. The real q range $-1 \le \cos(\sqrt{3}\,q/2) \le 1$ corresponds to the sinusoidal waves (46). These and only these non-localized waves can be radiated by the uniformly growing crack. Equation (47) yields two different functions for $\cos(\sqrt{3}\,q/2)$. So the corresponding plots consist of two branches. The plots for some speeds are presented in Figs. 12–16. Note that the gaps on the plots serve to separate the branches. In fact, the gaps do not exist, and, in each figure, the branches form a closed contour.

For the square lattice the main crack-speed-dependent direction of the radiation and the field asymptote are found based on the crack problem solution. At the same time, the main direction of the radiation, corresponding to the $n^{-1/3}$-asymptote, can also be determined based on the two-dimensional dispersion relation, without involving the complete solution. Indeed, from the sinusoidal wave representation (28) it follows that the exponent $\lambda = \exp(-iq)$, whereas the dispersion relation with $\omega = kv$ defines q as a function of k. In terms of the relation (37), $q = Q(k)$. The following considerations are the same as in Section 2.4. In this way, it can be shown that such critical points, $k = k_*(v)$, where $d^2Q(k)/dk^2 = 0$, also exist in the case of the triangular lattice.

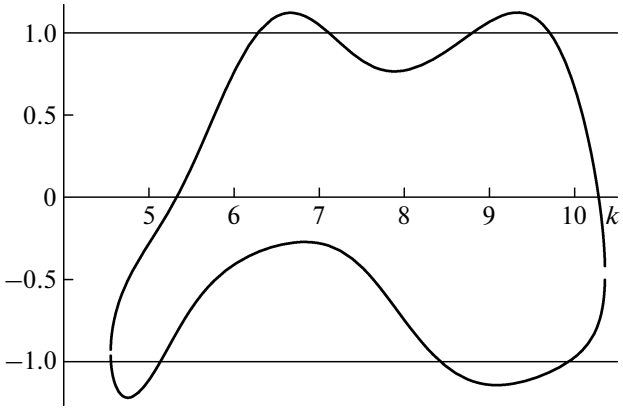

Fig. 12. The plot of $\cos(\sqrt{3}\,q/2)$ as a function of k based on (47) with $\omega = 0.4c_Rk$. The upper curve relates to ω_1, ω_2 (Fig. 10), the lower curve relates to ω_3, ω_4 (Fig. 11). The radiation wavenumbers correspond to real q, where $-1 \le \cos(\sqrt{3}\,q/2) \le 1$. The intersections of the curves with the lines ±1 correspond to the intersections of the ray $\omega = 04.c_Rk$ with the dispersion curves in Figs. 10, 11. The regions outside the ±1-strip correspond to complex q.

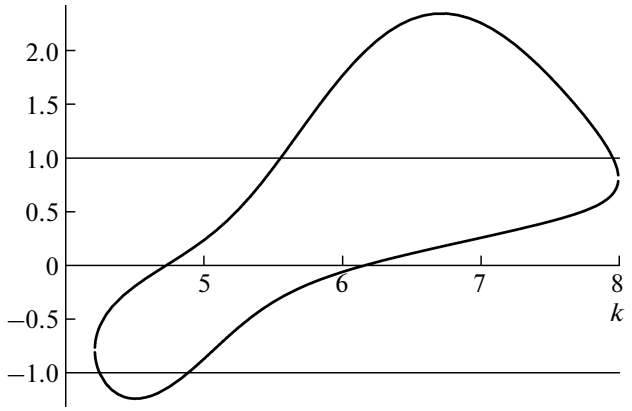

Fig. 13. Same as in Fig. 12, but for $\omega = 0.5c_R k$.

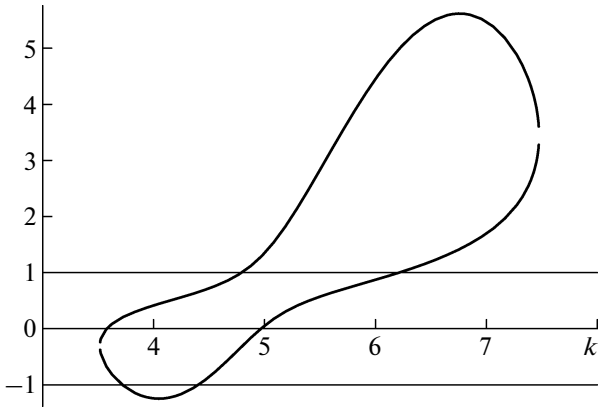

Fig. 14. Same as in Fig. 12, but for $\omega = 0.7c_R k$.

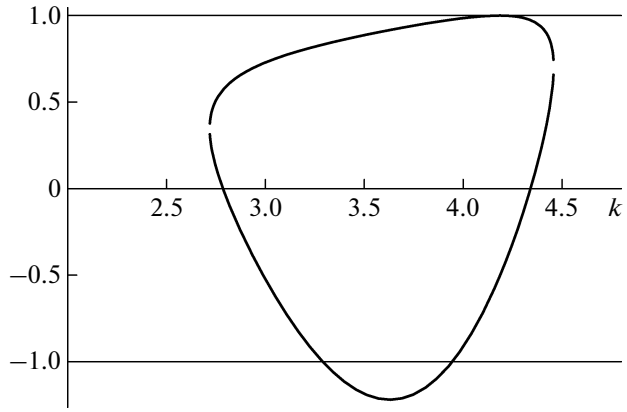

Fig. 15. Same as in Fig. 12, but for $\omega = 0.9c_R k$.

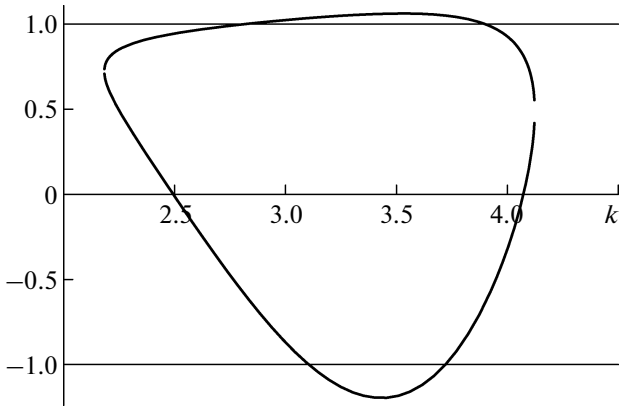

Fig. 16. Same as in Fig. 12, but for $\omega = c_R k$.

4. SOME CONCLUDING REMARKS

This article discusses the energy and structure of the waves radiated by a growing crack to the bulk of a lattice. The radiated energy is determined directly (23) (as it was done earlier for another situation in the article by Mishuris et al. (2009)). It is interesting that the same result was obtained by a completely different way, by comparing the exact solution for the crack line with its long-wave asymptote (Slepyan (1981a), see Section 2.2).

In the mode III fracture of the square lattice, the radiation is directed to the bulk of the lattice. In the plane problem for the triangular lattice, in addition, the lattice Rayleigh wave is excited. There exists the main crack-speed-dependent ray of the radiation, where the wave amplitude decreases most slowly. The asymptote is proportional to $n^{-1/3}$, and in a vicinity of this ray, the envelope is described by the Airy function.

A complete description of the wave structure can be extracted, in principle, from the crack problem solution, as it is done here for the square lattice. However, some important data concerning the wave radiation follow directly from the two-dimensional dispersion relations with the steady-state condition, $\omega = kv$ (see Section 3.4). First, the radiation wave-number segment, the $\mathfrak{K}$-segment, can be obtained, as it is done here for the triangular lattice. Next, it is the expression for the exponent, $\lambda(k) = \exp(-iq)$, where quantity q is defined by those relations as a function of k (here $k = k_x$, $q = k_y$). Thus the main crack-speed-dependent direction of the radiation and the normalized $n^{-1/3}$-asymptote are in hand (see (4), (28), (34) and (37)). Note that these lattice-associated phenomena cannot be observed in the classical elastic continuum, where the phase speed of a wave along a line cannot be low enough, $v \geq c_R$, and the crack uniformly growing with a subcritical speed does not radiate.

Finally note that the phenomena discussed in this paper are not confined to the crack problem. These phenomena are typical for the lattice under the action of a uniformly moving load.

REFERENCES

1. A. Cherkaev, E. Cherkaev, and L. Slepyan, J. Mech. Phys. Solids **53**, 383 (2005).
2. Sh. A. Kulakhmetova, V. A. Saraikin, and L. I. Slepyan, Mech. Solids **19**, 101 (1984).
3. G. S. Mishuris, A. B. Movchan, and L. I. Slepyan, J. Mech. Phys. Solids **57**, 1958 (2009), doi: 10.1016/j.jmps.2009.08.004.
4. L. I. Slepyan, Sov. Phys. Dokl. **26**, 538 (1981).
5. L. I. Slepyan, Sov. Phys. Dokl. **26**, 900 (1981).
6. L. I. Slepyan, *Models and Phenomena in Fracture Mechanics* (Springer, Berlin, 2002).
7. L. Slepyan and M. V. Ayzenberg-Stepanenko, J. Mech. Phys. Solids **52**, 1447 (2004).
8. L. I. Slepyan, A. Cherkaev, and E. Cherkaev, J. Mech. Phys. Solids **53**, 407 (2005).
9. L. I. Slepyan, G. S. Mishuris, and A. B. Movchan, Int. J. Fract. (2009), doi: 10.1007/s10704-009-9389-5.
10. L. I. Slepyan and L. V. Troyankina, J. Appl. Mech. Techn. Phys. **25**, 921 (1984).
11. A. Vainchtein, J. Mech. Phys. Solids **58**, 227 (2010).